Journal of Molecular Catalysis A: Chemical 338 (2011) 121–129

Contents lists available at ScienceDirect

Journal of Molecular Catalysis A: Chemical

journal homepage: www.elsevier.com/locate/molcata

Liquid and gas-phase Meerwein–Ponndorf–Verley reduction of crotonaldehyde on ZrO_2 catalysts modified with Al_2O_3, Ga_2O_3 and In_2O_3

Juan F. Miñambres, María A. Aramendía, Alberto Marinas, José M. Marinas, Francisco J. Urbano *

Department of Organic Chemistry, University of Córdoba, Campus de Rabanales, Marie Curie Building (Annex), E-14014 Córdoba, Spain

ARTICLE INFO

Article history:
Received 15 December 2010
Accepted 6 February 2011
Available online 12 February 2011

Keywords:
Zirconia based catalysts
Surface acidity
Surface basicity
Meerwein–Ponndorf–Verley reduction
Crotonaldehyde

ABSTRACT

A series of catalysts consisting of ZrO_2 modified with Al, Ga and In by coprecipitation with their precursor salts or impregnation of previously synthesized ZrO_2 with the nitrates of the metals was prepared. The solids thus obtained were characterized using a wide range or techniques including TG/DTG; XRD, SEM-EDAX, ICP-MS, FTIR and FT-Raman spectroscopies; and nitrogen adsorption–desorption at 77 K. The catalysts prepared by impregnation were found to contain Al, Ga and In nitrates while those obtained by coprecipitation contained Al_2O_3, Ga_2O_3 and In_2O_3. The catalysts were analyzed for surface acidity and basicity by thermal programmed desorption of pyridine and CO_2, respectively. The impregnated solids calcined at 300 °C exhibited low basicity and moderate acidity due to Brønsted and Lewis sites. The coprecipitated solids were slightly more acid and basic than their impregnated counterparts, their acidity being mainly due to the presence of Brønsted sites. Both types of solids were used as catalysts in the Meerwein–Ponndorf–Verley reduction of crotonaldehyde with 2-propanol as hydrogen donor. The impregnated solids calcined at 300 °C (particularly the Ga/ZrO_2 catalyst) were the most active and selective ones in the liquid phase reaction. The selectivity towards 2-butenol in the reaction in the gas phase was high at temperatures up to 250 °C, above which it dropped in a rapid manner. Again, the impregnated solids calcined at 300 °C were the most active and selective systems in the process (particularly Ga/ZrO_2).

1. Introduction

The reduction of carbonyl compounds by hydrogen transfer from an alcohol is known as the "Meerwein–Ponndorf–Verley reaction" or "MPV reaction" in Organic Chemistry. The presence of a C=C double bond conjugated with the C=O group in an α,β-unsaturated carbonyl compound introduces an additional dimension in the process: the chemoselective reduction of the C=O group in the presence of the C=C bond, which leads to the formation of an α,β-unsaturated alcohol (Scheme 1). This selective synthesis for primary and secondary alcohols is an important process for the pharmaceutical, fragrance and food flavouring industries. Their preparation by catalytic hydrogenation with a metal-supported catalyst is rather difficult owing to the high reactivity of the C=C bond relative to the carbonyl group [1]. However, the MPV reaction has been successfully used for the selective reduction of the C=O bond in α,β-unsaturated carbonyl compounds to the corresponding unsaturated alcohols [2,3].

Traditionally, the MPV reaction has been conducted using a metal (Al, Zr) alkoxide as catalyst in a homogeneous process. The reaction mechanism involves the formation of a six-membered cyclic intermediate where both reactants coordinate to the same metal site in the alkoxide [4–6]. The past two decades, however, have seen a rise in research aimed at facilitating conduct of the process in a heterogeneous phase on account of the major advantages of operating in this way in large-scale processes [5]. The reduction of α,β-unsaturated carbonyl compounds by hydrogen transfer under heterogeneous catalysis has so far been studied in the presence of a variety of catalysts including magnesium hydroxides [7], magnesium oxides [8–10], calcined hydrotalcites [11], hydrous and calcined zirconia [8,12,13], and a wide range of active components supported on zeolitic [4,14], mesoporous [15,16] and various other materials [17].

Although the mechanism behind these heterogeneous hydrogen transfer processes is seemingly quite clear, there remains some uncertainty as to the respective roles of surface acid (Lewis or Brønsted) and/or basic sites in the catalysts. Rather than a unified mechanism, researchers have proposed a number of them dependent on the particular catalyst used in the heterogeneous MPV reaction. Thus, the reduction of carbonyl compounds by hydrogen transfer has been hypothesized to occur at Lewis acid sites [4],

* Corresponding author. Tel.: +34 957218638; fax: +34 957212066.
E-mail address: FJ.Urbano@uco.es (F.J. Urbano).

1381-1169/$ – see front matter © 2011 Elsevier B.V. All rights reserved.
doi:10.1016/j.molcata.2011.02.005

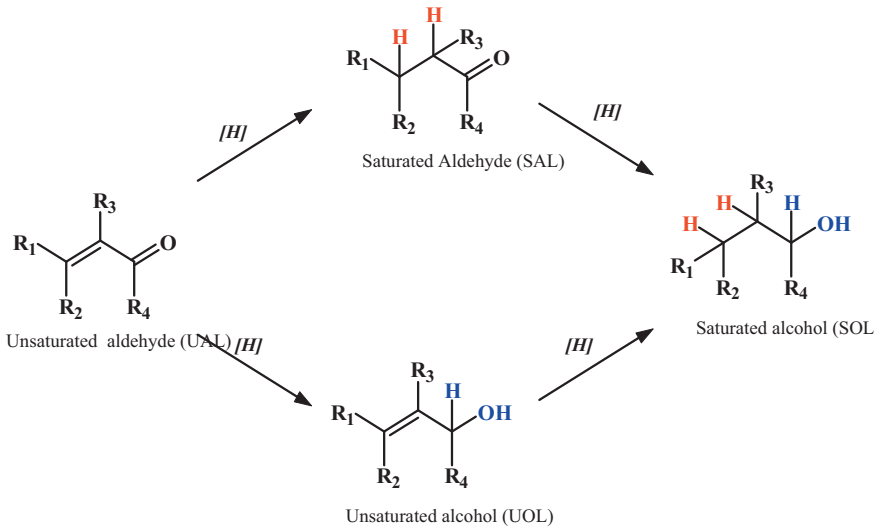

Scheme 1. Reaction network for the reduction of α,β-unsaturated carbonyl compounds.

Brønsted acid sites [12,13], basic sites [18,19] and acid–base pairs [10,20].

Zirconia has proved a highly effective choice among heterogeneous catalysts used in the MPV reaction [13]. Zirconium oxide is a solid with a high thermal stability and corrosion resistance in addition to a strong amphoteric character [21]. Textural and acid–base properties of ZrO_2 depend largely on its synthetic procedure and calcination temperature. Adjusting its acid–base properties is possible by modifying its surface with sulphate ions [22–24], phosphate ions [25] and mixtures of other oxides [3,26,27]; this has proved a highly effective method for tailoring the activity of zirconia towards many organic processes.

Some studies revealed catalytic activity in the MPV reaction to decrease with increasing calcination temperature (*i.e.* with increasing loss of surface hydroxyl groups) in hydrous zirconia; this underlines the significance of proton (Brønsted) sites to the process [12,13]. Moreover, it has been recently reported that the incorporation of boron into ZrO_2 leads to an increased catalytic activity in the liquid-phase MPV reduction of cinnamaldehyde consistent with an increased amount of highly strong proton (Brønsted) acid sites [3].

Modifying the surface chemical properties of ZrO_2 through the incorporation of Al_2O_3, Ga_2O_3 or In_2O_3 could allow to study the role of surface acid (Brønsted or Lewis) or basic sites on the activity and selectivity of the MPV reduction of crotonaldehyde with 2-propanol.

2. Experimental

2.1. Synthesis of catalysts

The studied catalysts were prepared by modifying zirconium oxide with 10% Al_2O_3, Ga_2O_3 or In_2O_3, either by coprecipitation with their precursor salts or by impregnation of previously synthesized pure ZrO_2, which was used as reference.

The reference zirconium oxide was obtained from zirconium oxychloride octahydrate (from Sigma–Aldrich). To this end, an appropriate amount of reagent was dissolved in 500 mL of water and precipitated by dropwise addition of 5 N NH_4OH to pH 9.5. The precipitate was allowed to stand overnight, filtered and washed with Milli-Q water as many times as required to give a negative chloride test with silver nitrate. The resulting solid was dried at 110 °C for 6 h, ground and sieved prior to calcination at 300 °C for 6 h, using a heating rate of 2 °C/min.

A similar procedure was used to obtain ZrO_2 catalysts modified with a 10 mol.% concentration of Al_2O_3, Ga_2O_3 or In_2O_3 by coprecipitation. The starting solution contained the corresponding precursors (*viz.* zirconium oxychloride and Al, Ga or In nitrate), appropriate amounts of which were dissolved in 500 mL of Milli-Q water and treated similarly as before. The resulting solids were also calcined at 175 or 300 °C for 6 h.

The reference zirconium oxide above described was split into four portions three of which were modified by impregnation with an aqueous solution of aluminium, gallium or indium nitrate (from Sigma–Aldrich). To this end, 6 g of ZrO_2 was suspended in 10 mL of Milli-Q water and supplied with the amount of nitrate needed to obtain a 10 mol.% concentration of the corresponding oxide in the final solid. The mixture was placed in a rotavapor for 2 h to obtain a homogeneous paste. Residual solvent was then evaporated by evacuation in a water bath at 60–80 °C. Once dry, the solid was calcined at 175 and 300 °C for 6 h, ground and sieved.

The catalysts were designated with the symbol for the zirconium-modifying element (Al, Ga or In), followed by that for the synthetic method used ("co" for coprecipitation and "im" for impregnation) and the calcination temperature used (175 or 300 °C). For example, the ZrO_2 catalyst containing 10 mol.% Al_2O_3, obtained by coprecipitation and calcined at 300 °C was designated Alco300.

2.2. Textural and structural characterization

Gels were subjected to thermogravimetric and differential thermal analysis on a Setaram Setsys 12 system, using Air at 40 mL/min as carrier gas, α-Al_2O_3 as reference material and a Pt/Pt–Rh (10%) thermocouple. The heating rate was 10 °C/min and the temperature range 30–1000 °C. The amount of gel used in each test was *ca.* 20 mg.

The textural properties of the solids were determined from nitrogen adsorption–desorption isotherms obtained at liquid nitrogen temperature on a Micromeritics ASAP-2010 instrument. All samples were degassed to 0.1 Pa at 110 °C prior to measurement. Surface areas were calculated using the Brunauer–Emmett–Teller (BET) method [28].

X-ray diffraction patterns were obtained on a Siemens D5000 diffractometer equipped with a graphite monochromator and using Co Kα radiation. The 2θ angle was scanned from 5 to 75° with a step size of 0.05°.

As far as EDX analyses are concerned, they were performed on a JEOL JSM-6300 SEM apparatus operating at an accelerating voltage of 20 keV with a resolution of 65 eV. EDX values corresponded to the average value of three measurements carried out at different areas of the solid with amplifications of 600 and 1000×.

The elemental analysis of the catalysts was performed on a Perkin–Elmer ELAN DRC-e ICP-MS instrument following digestion of the samples in a 1:1:1 mixture of HF, HNO_3 and H_2O, and dilution in 3% HNO_3. Calibration samples were prepared from appropriate atomic spectroscopy standards (PE Pure Plus, Perkin–Elmer) in HNO_3 (10 μg/mL of each metal). Calibration curves were constructed over the concentration range 1–100 ppb and included the results for a blank.

FT-IR spectra were recorded over a wavenumber range 400–4000 cm^{-1} on a Bomen MB-100 FT-IR spectrophotometer. The pellets were prepared by mixing the powdered solid with KBr in a 5:95 (w/w) ratio.

FT-Raman spectra were obtained on a Perkin–Elmer 2000 NIR FT-Raman system equipped with a diode pumped NdYAG laser (9394.69 cm^{-1}) that was operated at 300 mW laser power and a resolution of 4 cm^{-1} throughout the 3500–200 cm^{-1} range in order to gather 64 scans.

2.3. Surface acid–base properties

Acid–base properties were assessed by temperature-programmed desorption-mass spectrometry (TPD-MS) of pyridine (PY) for total acidity and CO_2 for total basicity. TPD-MS experiments were carried out on a Micromeritics TPD-TPR 2900 instruments fitted to a VG PROLAB Benchtop QMS (Thermo Scientific).

Pyridine was the probe molecule used to determine the acid properties of the catalysts. The base peak (m/z = 79) as well as a secondary one (m/z = 52, 80% abundance) was selected to be monitored in the mass spectrometer. Prior to the adsorption of the probe molecule, the catalyst (100 mg) was cleaned by passing an Ar stream (56 mL min^{-1}) up to 300 °C (at 10 °C min^{-1}) and cooling down in Ar to 30 °C. The solids were then saturated by passing an Ar stream (56 mL min^{-1}) at room temperature through a pure amine solution until complete saturation of the catalyst (about 30 min). Subsequently, a pure Ar stream (56 mL min^{-1}) was passed at the saturation temperature for 2 h in order to remove any physisorbed molecules. Once a stable line was obtained, chemisorbed PY was desorbed by heating from saturation temperature up to 300 °C in a programmed fashion, at a rate of 10 °C min^{-1}. The selected peaks were monitored through the whole process. Calibration was done by injecting pulses of variable size of a pyridine solution in cyclohexane. In parallel experiments, the solids saturated with PY, before being ramped, were analyzed *ex situ* by FT-Raman spectroscopy in order to distinguish between Brønsted (H-bonding or proton donor) or Lewis acid sites. The most sensitive Raman vibration of pyridine is its symmetric ring breathing (νCCN) (vs, v_1, A_1), which appears at 991 cm^{-1} in liquid pyridine. The interaction of pyridine with acid sites induces a shift in this band to a higher Raman Shift values. Therefore, the position of the skeletal vibration band can be used to detect interactions between pyridine and protonic weak acid sites through hydrogen bonds (996–1008 cm^{-1}) or its chemisorption at strong Brønsted (1007–1015 cm^{-1}) and/or Lewis acid sites (1018–1028 cm^{-1}) on a solid surface [29–31]. Spectra were collected as stated above and processed with the software PeakFit v. 4.11 in order to determine the components for physisorbed and chemisorbed pyridine in their three variants (hydrogen bonding interactions, Brønsted sites and Lewis sites).

Carbon dioxide (5% CO_2 in Argon) was the probe molecule used to determine the basic properties of the catalysts. The base peak (m/z = 44) as well as a secondary one (m/z = 12, 10% abundance) was selected to be monitored in the mass spectrometer. Prior to the adsorption of the probe molecule, the catalyst (100 mg) was cleaned by passing an Ar stream (56 mL min^{-1}) up to 300 °C (at 10 °C min^{-1}) and cooling down in Ar to 50 °C. The solids were then saturated by passing a CO_2/Ar stream (56 mL min^{-1}) at 50 °C. Subsequently, a pure Ar stream (56 mL min^{-1}) was passed at the saturation temperature for 2 h in order to remove any physisorbed molecules. Once a stable line was obtained, chemisorbed CO_2 was desorbed by heating from saturation temperature up to 300 °C in a programmed fashion, at a rate of 10 °C min^{-1}. The selected peaks were monitored through the whole process. Quantification was based on the 5% (v/v) CO_2/Ar standard.

2.4. Meerwein–Ponndorf–Verley reaction

The MPV reaction was conducted in both the liquid phase and the gas phase. Tests in the liquid phase were performed in a two-mouthed, round-bottom flask one mouth of which was used to introduce a 0.5 M solution of crotonaldehyde in isopropyl alcohol and 0.5 g of catalyst. The flask was fitted with a reflux condenser and placed in an ethyleneglycol bath that was kept at 130 °C throughout the reaction. The reaction medium was shaken in a continuous manner for 8 h and 0.2 mL aliquots were withdrawn from it at different times during the process and passed through a nylon filter of 0.45 μm pore size prior to analysis.

Tests in the gas phase involved using 50 mg of catalyst in a cylindrical reactor 10 mm in diameter that was placed in a tubular oven equipped with a 6-segment temperature controller. Prior to reaction, the solid was heated in a synthetic air stream at 300 °C for 30 min. Then, the catalyst was allowed to cool down to 200 °C (the reaction temperature). The reaction was started by replacing the synthetic air stream with a nitrogen stream flowing at 50 mL/min and carrying a 0.5 M solution of crotonaldehyde in isopropyl alcohol. The solution was injected at a rate of 1 g/h via a Bronkhorst High-Tech liquid mass flow controller and evaporated at 130 °C in a CEM mixer/evaporator (Bronkhorst High-Tech).

The above-described, isothermal tests were supplemented with others in the gas phase which were used to monitor catalyst activity and selectivity at variable temperatures from 150 to 300 °C obtained by heating at 10 °C/min. The highest temperature studied, 350 °C, was held for 30 min and followed by cooling down to 150 °C.

Products analysis was carried out on a Fisons Instruments GC 8000 Series gas chromatograph furnished with a 30 m long, 0.53 mm i.d. Supelcowax-10 semi-capillary column and fitted to a flame ionization detector (FID). The reaction products obtained for the crotonaldehyde (UAL) reduction were the crotyl alcohol (unsaturated alcohol, UOL), 1-butanol (saturated alcohol, SOL) and butanal (saturated aldehyde, SAL). The initial reduction rate of crotonaldehyde was expressed in terms of catalyst weight (g) and surface area (m^2) and the selectivity towards the unsaturated alcohol at variable conversion levels was calculated from the following expression:

$$S_{UOL} = (\text{mol crotyl alcohol/mol crotonaldehyde converted}) \times 100$$

3. Results and discussion

3.1. Textural and structural characterization of the catalysts

Table 1 shows the chemical composition and the most relevant textural, structural and surface chemical properties of the catalysts. Although their syntheses were conducted in such a way as to obtain a 10 mol.% concentration of modifying oxide, the ICP-MS results revealed that this theoretical content was never reached; in fact, the molar proportions of the oxides ranged from 3.4 to 5.6%

Table 1
Chemical composition (SEM-EDAX e ICP-MS) and textural (S_{BET}), structural (T_{GLOW}) and surface chemical (acid–base) properties of the synthesized catalysts.

Catalyst	DTA–T_{GLOW} (°C)	S_{BET} (m^2/g)	Chemical composition		Surface acidity		Surface basicity	
			SEM-EDAX (mol.%)	ICP-MS (mol.%)	Pyridine (μmol/g)	Pyridine (μmol/m^2)	CO_2 (μmol/g)	CO_2 (μmol/m^2)
Alco300	608	220	4.9	4.2	32.3	0.15	329	1.49
Gaco300	506	163	5.4	5.1	31.2	0.19	192	1.18
Inco300	445	173	4.0	5.6	22.7	0.13	302	1.75
Alim300	550	167	9.6	4.8	24.3	0.15	49	0.29
Gaim300	509	175	8.2	5.5	22.1	0.13	86	0.49
Inim300	459	161	6.3	3.4	20.2	0.13	64	0.40
ZrO_2	430	256	–	–	32.3	0.18	119	0.46
Alco175	608	276	4.9	4.2	–	–	–	–
Gaco175	506	215	5.4	5.1	–	–	–	–
Inco175	445	267	4.0	5.6	–	–	–	–
Alim175	550	136	9.6	4.8	–	–	–	–
Gaim175	509	167	8.2	5.5	–	–	–	–
Inim175	459	151	6.3	3.4	–	–	–	–

and were essentially similar in the coprecipitated and impregnated solids. The surface chemical data obtained by SEM-EDAX revealed more marked surface enrichment with Al, Ga or In in the impregnated solids than in their coprecipitated counterparts. Thus, the coprecipitated catalysts, consistent with the ICP-MS results, hardly reached 5 mol.% levels of the added oxides; by contrast, the impregnated catalysts exhibited increased surface concentrations of the oxides (particularly Alim and Gaim, with 9.6 and 8.2 mol.%, respectively) in greater consistency with the expected outcome for the ZrO_2 impregnation method.

All dry gels obtained immediately before calcination (*i.e.* all pre-catalysts) were subjected to thermogravimetry (TG–DTG) and thermal differential analysis (DTA). The TG–DTG results differed considerably between coprecipitated and impregnated catalysts. By way of example, Fig. 1 shows the thermal profiles for the precursor gels of the catalysts Alco and Alim.

The TG curves for the precursors revealed a similar weight loss (10–15%) in all solids. The curves exhibited two well-defined bands, namely: one at *ca.* 145 °C due to the loss of coordination water and leading to an amorphous zirconium hydroxide and the other, starting at 250 °C and ending at 400 °C, due to the gradual loss of hydroxyl groups to form an amorphous zirconium oxide [32]. Based on heat flow, all catalysts underwent an atomic rearrangement at *ca.* 400–600 °C by which the zirconium oxide gained structural order via crystallization. This reflected in an exothermic peak associated to no weight loss and known as "*glow exotherm*" the exact position of which is determined by the temperature of maximum exothermic flow, T_{GLOW} (Table 1) [32,33]. Crystallization in our pure ZrO_2 occurred at 430 °C; however, the presence of additives in the other solids raised T_{GLOW} (especially in the aluminium-containing solids). Based on the T_{GLOW} values of Table 1 and the calcination temperatures used (175 and 300 °C), the studied solids were amorphous in nature, as confirmed by the XRD results. In fact, the XRD patterns for both the coprecipitated catalysts and their impregnated counterparts contained no diffraction peaks or bands.

Also, the FT-Raman spectra (Fig. 2) provided virtually no useful information about the catalysts owing to their amorphous nature, which was previously confirmed by the XRD results. All spectra were essentially identical, the sole difference being the presence of a sharp peak at 1052 cm^{-1} for the impregnated catalysts that was assigned to the corresponding Al, Ga and In nitrates (see inset of Fig. 2). In fact, the nitrates incorporated into the zirconium oxide during the impregnation process must decompose only partly at the low–medium calcination temperature used (300 °C) and remain to some extent on the surface of the final catalyst. The absence of this sharp peak from the spectra for the coprecipitated catalysts can be ascribed to the supplied nitrates being completely transformed into hydroxides by precipitation with NH_4OH. The subsequent washing process removed the residual nitrates from the solids.

The infrared (FTIR) spectra for the catalysts were identical with one another and also with that for the reference zirconium oxide except for the presence of a strong band at 1385 cm^{-1} due to the presence of residual nitrate in the impregnated solids (Fig. 3), in agreement to the results obtained for FT-Raman. This assignation was confirmed by obtaining the FTIR spectra for aluminium gallium and indium nitrates calcined at 300 °C for 6 h (not shown). All other bands in the IR region were assigned to zirconium oxide. Thus, the broad band at 3400–3500 cm^{-1} was due to hydroxyl groups in the hydrated oxide and slightly weaker in the calcined solids, which,

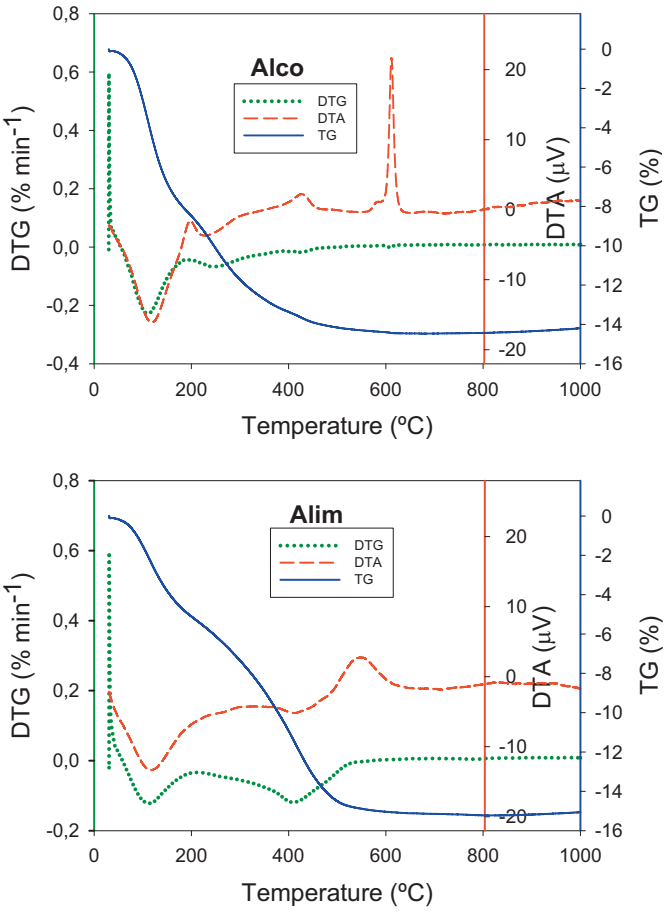

Fig. 1. TG/DTA profiles obtained for the Alco and Alim precursor gels.

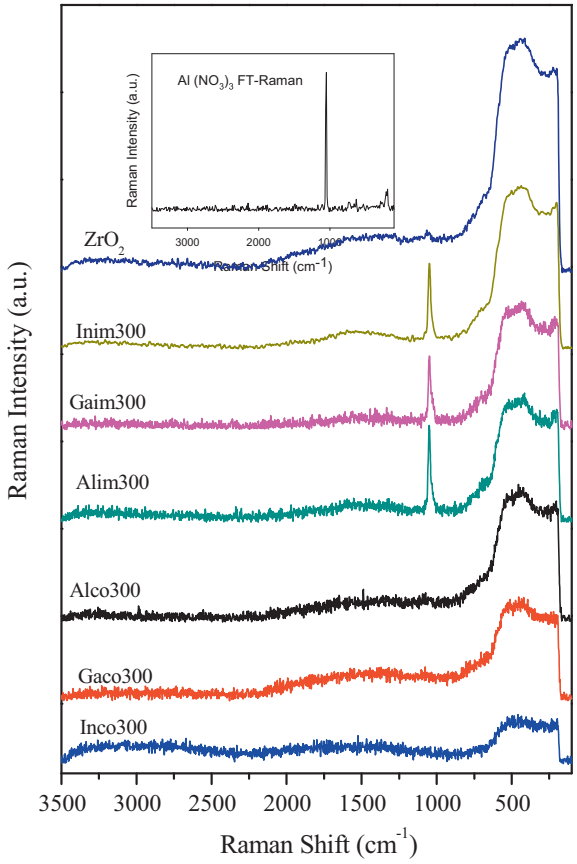

Fig. 2. FT-Raman spectra obtained for the catalyst synthesized in this work. The inset shows the FT-Raman spectrum obtained for the aluminium nitrate calcined at 300 °C for 3 h.

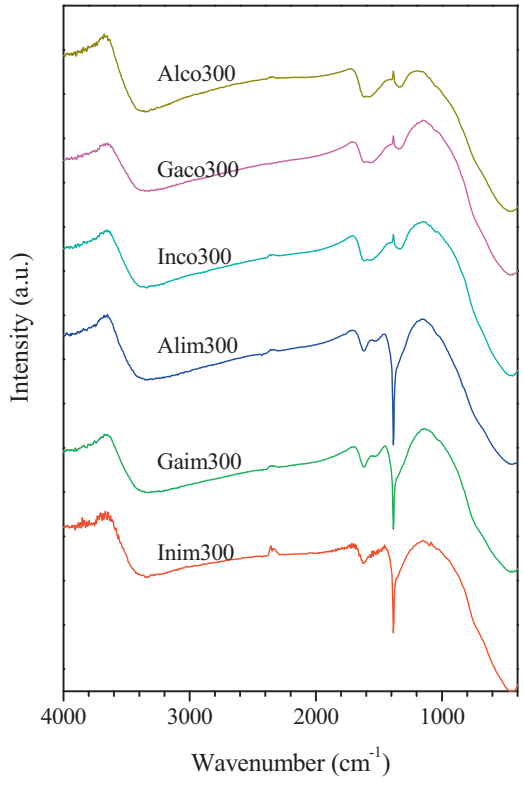

Fig. 3. FTIR spectra corresponding to the catalysts calcined at 300 °C.

consistent with the TG–DTG results, indicates the loss of OH groups upon calcination at 300 °C. The band at *ca.* 1600 cm^{-1} was assigned to atmospheric CO_2 adsorbed as bidentate carbonate. Finally, the strong, broad band at 470 cm^{-1} corresponded to Zr–O bonds. However, the typical band at 1000 cm^{-1} for Zr=O bonds was absent from the spectra, which indicates that the zirconium oxide was in the form of a polymer with its zirconium atoms linked by oxygen bonds [32].

As regard to textural properties, all isotherms obtained (results not shown) were of type IV in the IUPAC classification and exhibited an H2 hysteresis cycle associated to bottleneck pores. Based on pore size distribution, the average pore size was less than 50 Å.

The specific surface area of all solids calcined at 300 °C was essentially similar. By contrast, that of the solids calcined at 175 °C differed markedly. In fact, areas ranged from 161 m^2/g for Inim300 to 220 m^2/g for Alco300 among the former, and from 276 m^2/g for Alco175 to 136 m^2/g for Alim175 in the latter. Also, the solids modified with a given metal (Al, Ga or In) had greater surface areas when synthesized by coprecipitation than when obtained by impregnation – the opposite was only true for the Ga-modified catalysts calcined at 300 °C. It therefore seems obvious that impregnation of the reference ZrO_2 following calcination at 300 °C results in partial clogging of the pore network by the modifier and, consequently, in a decreased surface area relative to the support. On the other hand, the pore network in the coprecipitated solids forms after the modifier is structurally incorporated and the resulting specific surface area is greater – and close to that for the reference zirconium oxide – as a result.

3.2. Surface chemical properties of the catalysts

Surface acidity and basicity in the catalysts were determined by thermal programmed desorption of two different probes (pyridine and CO_2, respectively) following chemisorption at surface sites. Table 1 shows the surface acidity and basicity results obtained by integrating the areas under the pyridine and CO_2 desorption curves, respectively. The catalysts exhibited similar pyridine desorption profiles (not shown); pyridine desorption started around 70 °C and peaked at 140–150 °C. Based on the data of Table 1, Alco300, Gaco300 and ZrO_2 catalysts possessed the highest acidity per gram of solid. On the other hand, Inim300, Gaim300, Inco300 and Alim300 were the solids with the lowest surface acidity. The high surface area of Alco300 and, especially, the reference ZrO_2 resulted in a low surface acidity (per square meter) relative to Gaco300. Overall, the coprecipitated catalysts were more acid than their impregnated counterparts; this was particularly so with Alco300 and Gaco300. In fact, the impregnated solids were less acid than the reference ZrO_2.

The fact that the pyridine TPD profiles for the catalysts failed to clearly distinguish the presence of distinct types of acid sites led us to conduct an *ex situ* FT-Raman study of the solids following saturation with chemisorbed pyridine at exactly the point immediately preceding the start of the above-described thermal programmed desorption tests. Fig. 4 shows the FT-Raman signals for chemisorbed pyridine in the region of its symmetric ring-breathing vibration (vs, v1, A1). The interaction of pyridine with surface acid sites shifts the band to higher Raman wavenumbers. As a result, the position of the band can help to identify whether the interaction occurs via hydrogen bonds (996–1008 cm^{-1}) or with the pyridine chemisorbed at Brønsted (1007–1015 cm^{-1}) or Lewis acid sites (1018–1028 cm^{-1}) [31]. The most salient conclusion from this figure is that coprecipitated and impregnated catalysts differed in their acid sites. Thus, the impregnated solids (particularly Inim300) exhibited a strong component for Lewis acid sites at *ca.* 1021 cm^{-1} in addition to substantial Brønsted acidity (band at *ca.* 1007 cm^{-1}) and virtually no hydrogen-bonding interaction with

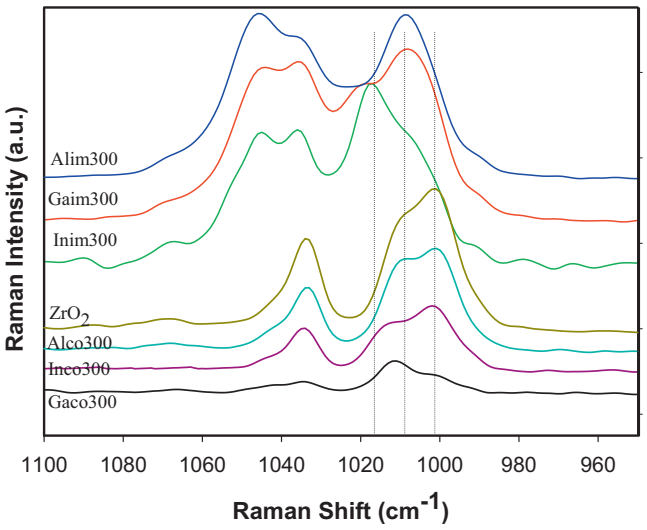

Fig. 4. FT-Raman spectra of pyridine chemisorbed over the catalysts calcined at 300 °C in the pyridine symmetric ring-breathing vibration region.

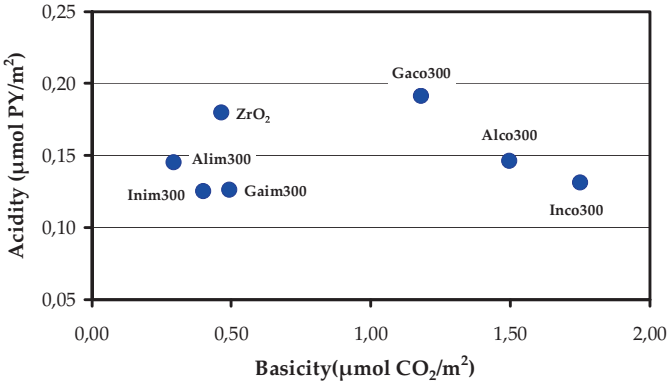

Fig. 5. Surface acid–base properties map corresponding to the catalysts used in this work.

pyridine. On the other hand, the coprecipitated catalysts and the reference zirconium oxide contained mostly Brønsted acid sites (band at *ca.* 1010 cm^{-1}) in addition to other, very weak acid sites that bound pyridine via hydrogen bonds (band at *ca.* 1000 cm^{-1}). As shown elsewhere, incorporating Ga into a mesoporous solid such as MCM-41 increases its acidity (particularly its Lewis acidity) [34].

The surface basic properties of the solids are summarized in Table 1. The TPD curves for CO_2 (not shown) were similar for all catalysts calcined at 300 °C. Desorption of the gas started at 60 °C in all and peaked at temperatures ranging from 100 °C for Inco300 to 150 °C for the reference ZrO_2. As can be seen from Table 1, the coprecipitated catalysts contained a significantly increased amount of basic surface sites per square meter of solid relative to the reference zirconium dioxide. The difference was greatest for Inco300, which trebled the basicity of the oxide. By contrast, the impregnated catalysts possessed a surface basicity per square meter of solid similar to that of the reference ZrO_2 except for the Alim300 that is slightly less basic. Unlike acidity, surface basicity differed markedly between the catalysts calcined at 300 °C (six times between the most basic solid, Inco300, and the least one, Alim300). The fact that, based on the FTIR and FT-Raman spectra, the impregnation method provided solids containing the modifying metal in nitrate form may somehow have restricted their basicity by effect of the absence of Al_2O_3, Ga_2O_3 and In_2O_3 from them.

Fig. 5 maps the surface acid–base properties of the catalysts. As can be seen, the impregnated catalysts were similar to the reference ZrO_2 as regard to such properties, the sole difference between the two being a slightly higher acidity in the latter; however, as shown by the FT-Raman spectra for chemisorbed pyridine, the acidity for impregnated solids was due to Lewis acid sites, which were absent from the reference ZrO_2. Finally, the basicity of the coprecipitated solids clearly exceeded that of the impregnated solids and the reference ZrO_2.

3.3. Catalytic activity

Following synthesis and characterization, the studied solids were used as catalysts in the Meerwein–Ponndorf–Verley (MPV) reaction of crotonaldehyde with 2-propanol as hydrogen donor. The chemoselective reduction to 2-butenol involved was studied in both the liquid and the gas phase.

The MPV reaction in the liquid phase (Table 2) exhibited moderate–low catalytic activity (conversion after 8 h was 5–26 mol.%) and a medium–high selectivity (44–88%) towards the unsaturated alcohol. In general, the results provided by the catalysts calcined at 175 °C were slightly worse than those obtained with the solids calcined at 300 °C. Also, the impregnated catalysts (particularly those calcined at 300 °C) clearly surpassed their coprecipitated counterparts in terms of activity and selectivity. The best results were those provided by Gaim300 (26% conversion and 86% selectivity towards 2-butenol), followed by Alim300 (21% conversion and 81% selectivity towards 2-butenol). As can be seen from Table 2, the average reaction rate after 8 h reaction was significantly lower than that after 2 h, which suggests that catalytic activity decreased as the reaction progressed. There was no clear-cut pattern of variation of the selectivity towards 2-butenol with time; some catalysts, however, exhibited a marked increase in selectiv-

Table 2
Liquid-phase MPV reduction of crotonaldehyde over the synthesized catalyst. Molar conversion (%Conv.), selectivity to the unsaturated alcohol ($\%S_{UOL}$) and reaction rate (per gram and per square meter) at two reaction times.

Catalyst	Reaction time: 2 h				Reaction time: 8 h			
	%Conv.	$\%S_{UOL}$	r_g (μmol/min g)	r_S (μmol/min m^2)	%Conv.	$\%S_{UOL}$	r_g (μmol/min g)	r_S (μmol/min m^2)
Alco175	8	77	15.8	0.057	8	78	3.8	0.014
Inco175	3	77	5.8	0.022	5	79	2.4	0.009
Gaco175	6	85	11.5	0.053	7	51	3.3	0.015
Alim175	8	77	15.8	0.116	8	77	4.2	0.031
Inim175	4	76	7.4	0.049	9	79	4.4	0.029
Gaim175	5	100	10.0	0.060	15	87	7.7	0.046
Alco300	4	4	7.3	0.033	5	44	2.4	0.011
Inco300	4	16	8.4	0.049	5	46	2.4	0.014
Gaco300	3	31	5.1	0.031	8	88	4.0	0.025
Alim300	10	68	20.1	0.120	21	81	10.3	0.061
Inim300	5	90	9.6	0.060	12	87	5.8	0.036
Gaim300	11	71	22.2	0.127	26	86	12.9	0.074

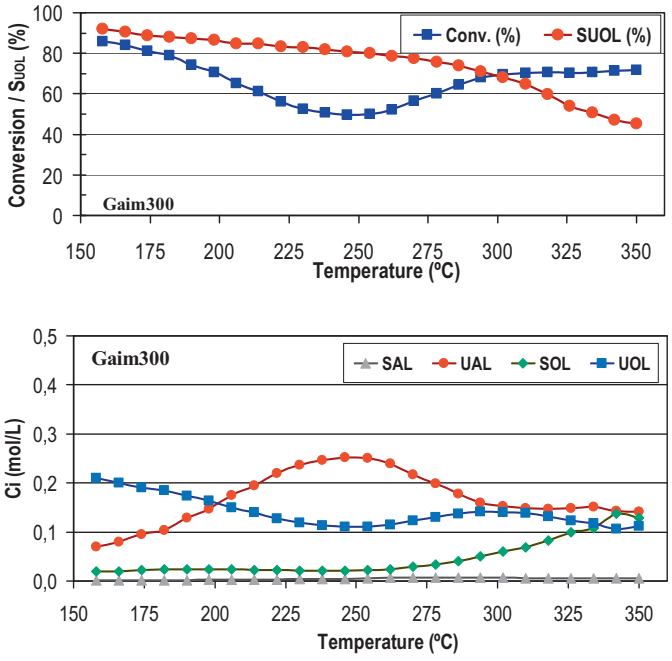

Fig. 6. Temperature-programmed gas-phase MPV reduction of crotonaldehyde over Gaim300 catalyst. Reaction temperature was ramped from 150 °C to 350 °C at 10 °C/min.

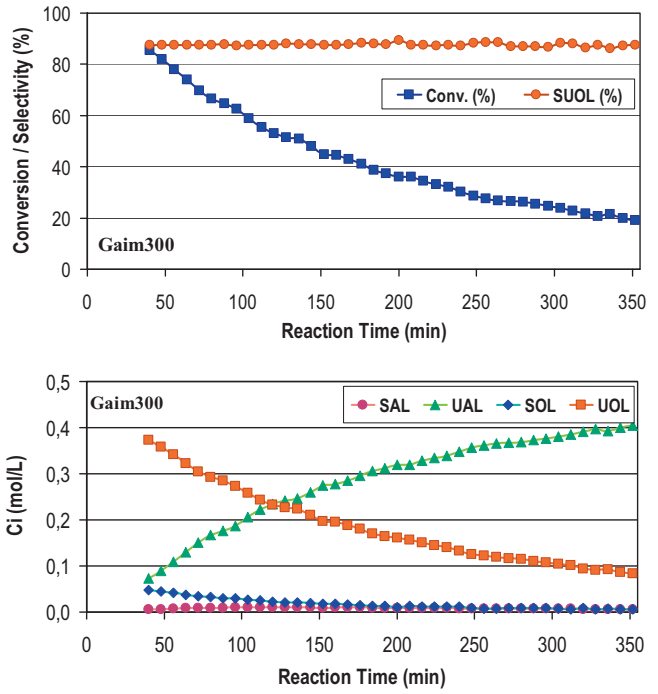

Fig. 7. Isotherm gas-phase MPV reduction of crotonaldehyde over Gaim300 catalyst at 200 °C.

ity with time, particularly those calcined at 300 °C. This suggests that the loss of selectivity to unsaturated alcohol was more marked in the initial reaction segment by the formation of 1-butanol and that deactivation was greater at the active sites producing that saturated alcohol. The activity loss was stronger in the solids calcined at 175 °C – Gaim175 excepted – and in the coprecipitated solids calcined at 300 °C. By contrast, the impregnated solids calcined at 300 °C exhibited an increased ability to retain their catalytic activity.

The reaction tests in the gas phase were initially conducted using a temperature ramp in order to obtain an overview of catalytic performance over a wide temperature range (150–350 °C). In any case, the conclusions thus drawn are subject to the potential influence of deactivation processes at high temperatures and the fact that the highest temperature was 50 °C higher than that of calcination of the solids. By way of example, Fig. 6 shows the results for catalyst Gaim300 and Table 3 summarizes the results derived from the profiles for the body of catalysts at four different temperatures. For all catalysts, the results were essentially similar. Thus, some catalysts were already active at 150 °C – some, such as Alco300, Alim300, Gaim300 and Inim300, highly active. The reference ZrO_2 was also active at 150 °C, but all other catalysts exhibited minimal activity at the lower end of the temperature range. However, some of the more active catalysts at 150 °C rapidly lost activity by effect of a severe deactivation process as the temperature was raised. Such was the case with Alim300, Gaim300 and Inim300, which, interestingly, were all obtained by impregnation. Solid Alco300, however, provided a conversion of *ca.* 50% at 200 °C that increased gradually with increasing temperature; also, it exhibited no signs of severe deactivation throughout the rest of the test (*viz.* up to 350 °C, where it provided 100% conversion). However, the selectivity of this catalyst for 2-butenol dropped to levels in the region of 10% at high temperatures, where 1-butanol was the dominant product. Butanal levels with this catalyst were minimal throughout the studied temperature range; this suggests that the solid allows reduction of the C=C bond in 2-butenol to give 1-butanol but not that of the C=C bond in crotonaldehyde to give butanal. Previous studies of the dehydration/dehydrogenation of 2-propanol on ZrO_2 revealed that the dehydrogenation of the alcohol to acetone and molecular hydrogen occurs at high temperatures (above 300 °C) [35] and also that the C=C bond is reduced by H_2 produced in the reaction. The reduction of the C=O bond must, however, require hydrogen transfer from the alcohol to the carbonyl group via a previously reported cyclic intermediate [2,5]. The other catalysts exhibited similar reaction profiles irrespective of the conversions levels obtained at the different temperatures studied. Thus, the selectivity towards 2-butenol was very high (>70%) at medium–low temperatures (below 250 °C), but fell by effect of the formation of 1-butanol at higher temperatures. In any case, butanal was never produced at levels exceeding 4–5%.

Based on the previous results, we chose a temperature of 200 °C for an isothermal study of the MPV reaction in the gas phase, using all catalysts calcined at 300 °C. By way of example, Fig. 7 illustrates the performance of solid Gaim300 in the process, and Table 4 shows the molar conversion, selectivity towards the unsaturated alcohol and reaction rate in the MPV reduction of crotonaldehyde in the gas phase at 200 °C after 80 and 335 min reaction. All catalysts proved active – albeit with large differences in crotonaldehyde conversion – at the shorter reaction time (80 min). Thus, the coprecipitated solids provided conversions from 4% (Inco300) to 16% (Alco300), whereas their impregnated counterparts resulted in much higher levels ranging from 42% with Inim300 to 67% with Gaim300. On

Table 3
Temperature-programmed gas-phase MPV reduction of crotonaldehyde over the catalysts calcined at 300 °C. Molar conversion (%Conv.) and selectivity to the unsaturated alcohol ($\%S_{UOL}$) at four reaction temperatures.

Catalyst	200 °C		250 °C		300 °C		350 °C	
	%Conv.	$\%S_{UOL}$	%Conv.	$\%S_{UOL}$	%Conv.	$\%S_{UOL}$	%Conv.	$\%S_{UOL}$
Alco300	49	79	68	74	91	40	100	10
Gaco300	15	87	28	78	56	66	79	47
Inco300	15	83	21	81	52	66	87	37
Alim300	51	87	36	75	42	59	66	38
Gaim300	70	86	50	80	69	68	73	46
Inim300	38	84	23	80	30	64	28	64
ZrO_2	16	83	27	78	60	92	96	34

Table 4
Isotherm gas-phase MPV reduction of crotonaldehyde (at 200 °C) over the catalysts calcined at 300 °C. Molar conversion (%Conv.), selectivity to the unsaturated alcohol ($\%S_{UOL}$) and reaction rate (per gram and per square meter) at two reaction times.

Catalyst	Reaction time: 80 min				Reaction time: 335 min			
	%Conv.	$\%S_{UOL}$	r_g (μmol/min g)	r_S (μmol/min m^2)	%Conv.	$\%S_{UOL}$	r_g (μmol/min g)	r_S (μmol/min m^2)
Alco300	16	83	34.0	0.123	0	0	0.0	0.000
Inco300	4	87	8.4	0.032	0	0	0.0	0.000
Gaco300	6	80	13.2	0.061	0	0	0.0	0.000
Alim300	63	88	133.5	0.981	14	88	30.1	0.221
Inim300	42	86	89.5	0.591	9	88	19.1	0.126
Gaim300	67	87	141.4	0.848	21	86	45.5	0.273

the other hand, selectivity was similar with all catalysts and ranged from 80% with Gaco300 to 88% with Alim300. The longer reaction time (335 min) resulted in substantial deactivation of the catalysts (particularly the coprecipitated solids, which lost all activity within 5 h). The impregnated catalysts also exhibited strong deactivation; however, they retained some of their high initial conversions and led to final values ranging from 9% for Inim300 to 21% for Gaim300. Unlike the liquid phase, deactivation of the catalysts with the reactants in the gas phase had no effect on the selectivity towards the unsaturated alcohol, which remained as high as 86–88%. The best results in the MPV reduction of crotonaldehyde in the gas phase at 200 °C were those obtained with Gaim300, which exhibited 21% conversion and 86% selectivity for 2-butenol after 5 h reaction. This was also the best performing catalyst in the liquid phase, where it provided 26% conversion and 86% selectivity. Catalyst Gaim300 was followed in performance by the other two impregnated solids calcined at 300 °C (Alim300 and Inim300). This suggests that the impregnation method provides more active and at least as selective catalysts as the coprecipitation method.

As noted earlier, the impregnated solids calcined at 300 °C had a low surface basicity and a moderate surface acidity (Table 1). However, the FT-Raman spectra for pyridine chemisorbed on the impregnated catalysts revealed the presence of a substantial proportion of pyridine adsorbed at Lewis acid sites, which were absent from the coprecipitated solids and the reference ZrO_2. Also, as revealed by the FTIR and FT-Raman spectra, the impregnated catalysts calcined at 300 °C contained nitrate and its presence seemingly led to the formation of Lewis acid sites, which are highly active in the MPV reaction [36]. The research conducted in this work could be expanded in the future by studying the mechanisms by which the studied catalysts are deactivated and whether their deactivation is related to the presence of any specific type of acid or basic site.

4. Conclusions

In this work, we synthesized zirconium oxide catalysts modified with aluminium, gallium or indium by impregnation or coprecipitation. The solids thus prepared were characterized and used as catalysts in the MPV reduction of crotonaldehyde in the liquid and gas phase. The results obtained allow us to draw the following conclusions:

(a) The solids produced by the impregnation method contain Al, Ga or In nitrate that is incompletely decomposed by calcining at 300 °C. This is not the case with the coprecipitated solids, which consist of ZrO_2 and Al_2O_3, Ga_2O_3 or In_2O_3. All solids are amorphous and possess a high specific surface area.
(b) Based on surface chemical properties, the impregnated solids calcined at 300 °C possess a low basicity and a moderate acidity. However, the FT-Raman spectra for pyridine chemisorbed on them revealed that a substantial proportion of the probe molecule was adsorbed at Lewis acid sites and that such was the case with neither the coprecipitated solids nor the reference ZrO_2. The coprecipitated solids are slightly more basic, and also slightly more acid, than the impregnated solids; the increased acidity, however, is due to Brønsted sites of medium and low strength some of them only interacting with pyridine through hydrogen bonding.
(c) The most active catalysts in the MPV reduction of crotonaldehyde in both liquid and gas phase are those obtained by impregnating ZrO_2 with Al, Ga or In nitrate. Specifically, Gaim300 proved the most active solid in the process. All catalysts are very selective (80–88%) towards the unsaturated alcohol in the gas-phase process conducted at 200 °C.
(d) The catalysts are deactivated in the process, both in the liquid phase and in the gas phase. However, the loss of activity in the liquid phase is accompanied by an increase in selectivity towards 2-butenol, whereas that in the gas phase has no such effect on selectivity.

Acknowledgments

The authors are thankful to MICINN (Projects CTQ2008/01330 and CTQ2010/18126), Junta de Andalucia (P07-FQM-02695, P08-FQM-3931, and P09-FQM-4781) and FEDER funds for financial support. The Central Services (SCAI) at the University of Cordoba are also acknowledged.

References

[1] P. Maki-Arvela, J. Hajek, T. Salmi, D.Y. Murzin, Appl. Catal. A 292 (2005) 1–49.
[2] J.R. Ruiz, C. Jimenez-Sanchidrian, Curr. Org. Chem. A 11 (2007) 1113–1125.
[3] F.J. Urbano, R. Romero, M.A. Aramendia, A. Marinas, J.M. Marinas, J. Catal. 268 (2009) 79–88;
F.J. Urbano, R. Romero, M.A. Aramendia, A. Marinas, J.M. Marinas, J. Catal. 271 (2010) 153.
[4] E.J. Creyghton, R.S. Downing, J. Mol. Catal. A 134 (1998) 47–61.
[5] G.K. Chuah, S. Jaenicke, Y.Z. Zhu, S.H. Liu, Curr. Org. Chem. A10 (2006) 1639–1654.
[6] A. Corma, S. Iborra, Adv. Catal. Vol. 49 (2006) 239–302.
[7] M.A. Aramendia, V. Borau, C. Jimenez, J.M. Marinas, J.R. Ruiz, F.J. Urbano, J. Mol. Catal. A 171 (2001) 153–158.
[8] F. Braun, J.I. Di Cosimo, Catal. Today 116 (2006) 206–215.
[9] J.I. Di Cosimo, A. Acosta, C.R. Apesteguia, J. Mol. Catal. A 234 (2005) 111–120.
[10] J.I. Di Cosimo, A. Acosta, C.R. Apesteguia, J. Mol. Catal. A 222 (2004) 87–96.
[11] M.A. Aramendia, V. Borau, C. Jimenez, J.M. Marinas, J.R. Ruiz, F. Urbano, Appl. Catal. A 249 (2003) 1–9.
[12] Y. Zhu, S. Liu, S. Jaenicke, G. Chuah, Catal. Today 97 (2004) 249–255.
[13] S.H. Liu, S. Jaenicke, G.K. Chuah, J. Catal. 206 (2002) 321–330.
[14] Y. Zhu, G.K. Chuah, S. Jaenicke, J. Catal. 241 (2006) 25–33.
[15] A. Ramanathan, M.C. Castro Villalobos, C. Wakernaak, S. Telalovic, U. Hanefeld, Chem. Eur. J. 14 (2008) 961–972.
[16] A. Ramanathan, D. Klomp, J.A. Peters, U. Hanefeld, J. Mol. Catal. A 260 (2006) 62–69.
[17] S. Nishiyama, M. Yamamoto, H. Izumida, S. Tsuyura, J. Chem. Eng. Jpn. 37 (2004) 310–317.
[18] M. Berkani, J.L. Lemberton, M. Marczewski, G. Perot, Catal. Lett. 31 (1995) 405–410.
[19] J. Lopez, J.S. Valente, J.-M. Clacens, F. Figueras, J. Catal. 208 (2002) 30–37.
[20] V. Ivanov, J. Bachelier, F. Audry, J.C. Lavalley, J. Mol. Catal. 91 (1994) 45–59.

[21] K. Tanabe, T. Yamaguchi, Catal. Today 20 (1994) 185–197.
[22] C.J. Zhang, R. Miranda, B.H. Davis, Catal. Lett. 29 (1994) 349–359.
[23] F. Lonyi, J. Valyon, J. Therm. Anal. 46 (1996) 211–218.
[24] K. Arata, Appl. Catal. A 146 (1996) 3–32.
[25] D. Spielbauer, G.A.H. Mekhemer, T. Riemer, M.I. Zaki, H. Knozinger, J. Phys. Chem. B 101 (1997) 4681–4688.
[26] K.M. Malshe, P.T. Patil, S.B. Umbarkar, M.K. Dongare, J. Mol. Catal. A 212 (2004) 337–344.
[27] B.Q. Xu, S.B. Cheng, X. Zhang, Q.M. Zhu, Catal. Today 63 (2000) 275–282.
[28] S. Brunauer, P.H. Emmett, E.J. Teller, J. Am. Chem. Soc. 60 (1938) 309–319.
[29] A.A.M. Ali, M.I. Zaki, Colloid Surf. A 139 (1998) 81–89.
[30] R. Burch, C. Passingham, G.M. Warnes, D.J. Rawlence, Spectrochim. Acta A 46 (1990) 243–251.
[31] M.A. Aramendia, V. Borau, C. Jimenez, J.M. Marinas, J.R. Ruiz, F.J. Urbano, J. Colloid Interface Sci. 217 (1999) 186–193.
[32] G.Y. Guo, Y.L. Chen, J. Mater. Sci. 39 (2004) 4039–4043.
[33] G.K. Chuah, S. Jaenicke, B.K. Pong, J. Catal. 175 (1998) 80–92.
[34] J.M. Campos, J.P. Lourenço, A. Fernandes, A.M. Rego, M.R. Ribeiro, J. Mol. Catal. A 310 (2009) 1–8.
[35] M.A. Aramendia, V. Borau, C. Jimenez, J.M. Marinas, A. Porras, F.J. Urbano, J. Chem. Soc. Faraday Trans. 93 (1997) 1431–1438.
[36] M. Boronat, A. Corma, M. Renz, J. Phys. Chem. B 110 (42) (2006) 21168–21174.